REPORT DOCUMENTATION PAGE

Form Approved OMB No. 0704-0188

1. AGENCY USE ONLY (Leave blank)	2. REPORT DATE 1997	3. REPORT TYPE AND DATES COVERED Final Report

4. TITLE AND SUBTITLE

Dynamic Dual-Frequency Control of Nematic Liquid Crystals in Adaptive Optics Systems

5. FUNDING NUMBERS

F6170897W0047

6. AUTHOR(S)

Dr. Alexandre Naoumov

7. PERFORMING ORGANIZATION NAME(S) AND ADDRESS(ES)

Laser Measuring Branch, P. N. Lebedev Physical Institute, Samara Branch
Novo-Sadovaja St. 221
Samara 443011
Russia

8. PERFORMING ORGANIZATION REPORT NUMBER

N/A

9. SPONSORING/MONITORING AGENCY NAME(S) AND ADDRESS(ES)

EOARD
PSC 802 BOX 14
FPO 09499-0200

10. SPONSORING/MONITORING AGENCY REPORT NUMBER

SPC 97-4015

11. SUPPLEMENTARY NOTES

12a. DISTRIBUTION/AVAILABILITY STATEMENT

Approved for public release; distribution is unlimited.

12b. DISTRIBUTION CODE

A

13. ABSTRACT (Maximum 200 words)

This report results from a contract tasking Laser Measuring Branch, P. N. Lebedev Physical Institute, Samara Branch as follows: The contractor will investigate dual-frequency control of liquid crystals in order to establish limits on rise and fall times as outlined in the proposal. He will also investigate control methods for liquid crystal modulators. The contractor will design and construct a programmable generator that he will use to study the possibility of improving the response time of liquid crystal modulators by controlling the voltage time history.

19980102 016

DTIC QUALITY

14. SUBJECT TERMS

Atmospherics, Optical Components, Non-linear Optics, Materials

15. NUMBER OF PAGES

52

16. PRICE CODE

N/A

17. SECURITY CLASSIFICATION OF REPORT	18. SECURITY CLASSIFICATION OF THIS PAGE	19. SECURITY CLASSIFICATION OF ABSTRACT	20. LIMITATION OF ABSTRACT
UNCLASSIFIED	UNCLASSIFIED	UNCLASSIFIED	UL

RUSSIAN ACADEMY OF SCIENCE

P.N.LEBEDEV PHYSICAL INSTITUTE

SAMARA BRANCH

FINAL REPORT

for European Office of Aerospace Research and Development (EOARD)

contract No F61708-97-W0047

DYNAMIC DUAL-FREQUENCY CONTROL
OF NEMATIC LIQUID CRYSTALS IN ADAPTIVE
OPTICS SYSTEMS

SPC 97-4015

EXECUTORS

A.F.Naumov

V.N.Belopukhov

SAMARA – 97

1. INTRODUCTION

The real-time wavefront controlled shaping problems are important in modern science and technology. The fine-scale atmospheric phase distortions' compensation is one of them. Cost and complexity of control limit use of traditional adaptive mirrors with electromechanical drivers. At the same time, liquid crystal spatial phase light modulator can be able to solve this problem. However, it is necessary to include the features of control of liquid crystal wavefront correctors in closed adaptive systems. The amplitude control used in adaptive systems with deformable mirrors is not acceptable for fast liquid crystal adaptive systems. Furthermore, liquid crystal correctors are non-linear electrooptic elements and this circumstance should be taken into account when designing the feedback circuit.

The work proposed here is aimed to provide data on dynamic dual-frequency control in adaptive systems taking into account the adaptive optics specific of the liquid crystal application. These data would be useful to the Phillips Laboratory when designing and constructing the next generation of liquid crystal devices for adaptive optics.

Our enduring investigations in the liquid crystal adaptive optics and significant successes by Phillips Laboratory's collaborators in the same field induced this work supported by Dr. John K. McIver form EOARD.

However, we would be like to note that the complete system analysis problems exceed the bounds of this project. We hope to solve the problems of optimal control selection and of feedback stability in closed adaptive systems in the nearest future by means of the equipment that we are designing now.

2. ABSTRACT

The commercially available liquid crystal light valves were developed in the middle of 1970s and had been extensively used for display applications [1], and later for laser optics [2,3] and for radar applications [4] instead of the solid-crystalline materials, which could not be used in large aperture optical devices.

Significant success in the field of synthesis and research of liquid crystals attracts attention because of wide potential opportunities: low control voltage 1...100V, small consumed capacities ~0,1mw/cm^2, small volume of a flat design, opportunity of construction of devices with the large aperture for transmitted light controlling, wide interval of working temperatures are characteristic: -20...100°C, low cost of initial materials, simplicity of manufacturing, significant service life more than 10^4 h. The specified features allow to consider liquid crystal as rather perspective materials for wavefront correctors in adaptive optics. However, one limitation exists - its temporal bandwidth. Attempts to overcome this limitation were connected with creation of devices with very thin liquid crystal layers, special modulators design for high voltage control, increase of temperature, selection of liquid crystal materials and dual frequency control. The short review of these methods will be given later.

Having overcome the ferroelectric alignment problem, a new possibility for design of very fast modulators and for investigation of ferroelectric crystals was discovered. The primary attraction of modulators based on ferroelectric liquid crystals is the much higher speed potential compared to nematic liquid crystals. The observed response times for the ferroelectric liquid crystal materials can be submicrosecond [5] for a binary-only polarization or intensity modulation. Ferroelectric modulators can be used for continuous phase-only modulation, although in very small region up to π only. The unusual regime of control is due to a very small feeding voltage and, therefore, these modulators have a low rapidity (283µs for 0.5V/µ [6]). The interesting method was suggested in [7]. The discrete eight-level phase modulation is achieved by cascading of three binary-only phase modulators, one $\lambda/2$ and

two $\lambda/4$ retarders and four linear polarizers. Evidently, this method is not suitable for atmosphere wavefront correctors because of complexity.

So, among various types of liquid crystals only nematic liquid crystals are available for our research.

The dynamics of nematic liquid crystals was intensively studied about twenty years ago. At that time liquid crystals were not used in adaptive optics because not all resources of deformable mirrors were exhausted. Now the situation has changed. Already there are a high technology of manufacturing liquid crystal devices and hardware for their control, and the dynamics of nematics represents an interest again. We are going to summarize all the results and include all possible limitations, and then we will propose different control methods.

2. DYNAMICS AND USEFUL APPROXIMATIONS

A liquid crystal material is an anisotropic medium that can be treated locally as a uniaxial crystal whose optical axis is parallel to the director of the molecules (domains). Here we will regard nematic liquid crystals with a homogeneous initial orientation of the director and with initial positive anisotropy of the dielectric permittivity. Fig. 1 shows a scheme of such liquid crystal cell, a thin layer of liquid crystal *1* is sandwiched between two parallel glass plates *2*, onto which transparent electrodes *3* are deposited. The surfaces of the electrodes are coated with liquid crystal aligning films *4*. When no electrical field is applied, the liquid crystal molecules have homogeneous orientation. If a modulating electric field is applied across the liquid crystal layer through the transparent electrodes, the crystal molecules turn lengthwise along the field. Because the effective refractive index of the liquid crystal depends on the angle of the molecules relative to the direction of incident light, the phase of light transmitted through the liquid crystal cell can be controlled by the applied electrical field. Phase delay between extraordinary and ordinary components of passing light wave through the liquid crystal layer
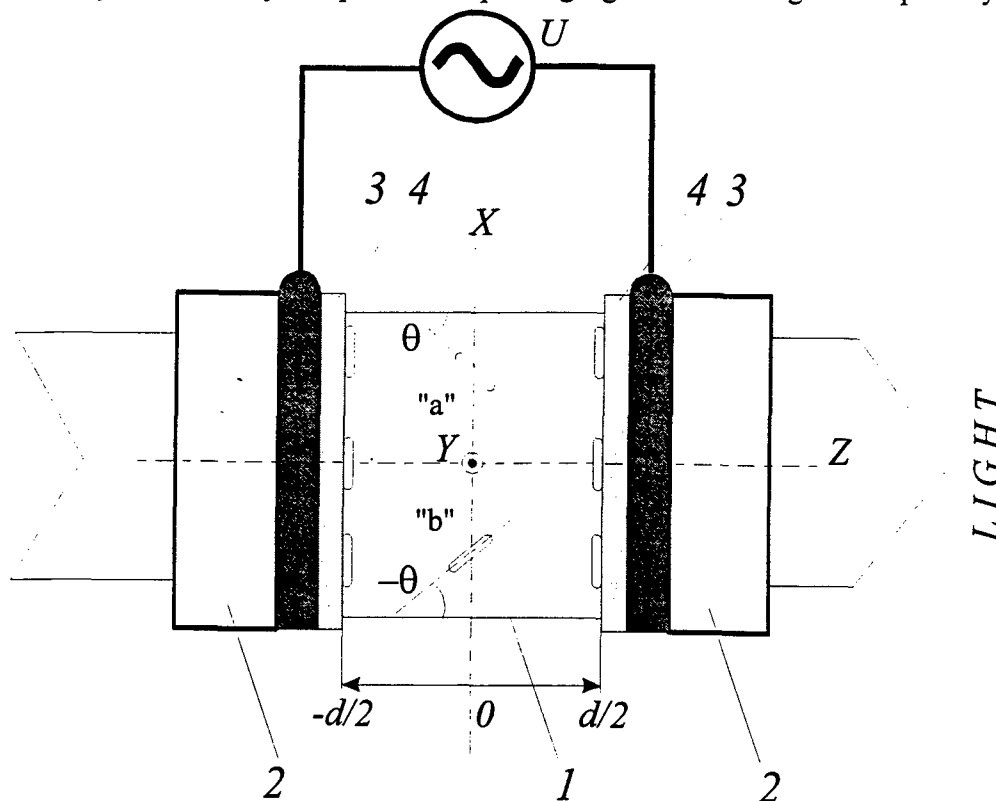

Fig. 1. Nematic liquid crystal cell with homogeneous orientation on substrates.

is determined by orientation of molecules in this layer:

$$\Delta\Phi = \frac{2\pi}{\lambda} \int\limits_{-d/2}^{d/2} \left[n(z) - n_\perp \right] dz ,$$ (1)

where $n(z)$ is the liquid crystal refractive index, which can be varied from $n_\parallel$ up to $n_\perp$, d is the thickness of the layer and λ is wave length. The indices $n_\parallel$ and $n_\perp$ accord to the measured index along and normal to initial orientation of the director. We assume the passing light wave to be monochromatic and linear-polarized in the initial orientation direction of the liquid crystal, although the later is not important usually [8].

Let's evaluate the cell birefringence dynamic behavior. Theoretical analysis of liquid crystal birefringence is connected with solving the Oseen-Frank's equation [9] for elastic energy density, dielectric displacement energy density, and an energy dissipation density that is reduced to Ericksen-Leslie's equation [10]:

$$\frac{\partial}{\partial z}\left[\left(K_{11} \cos^2\theta + K_{33} \sin^2\theta \right) \frac{\partial\theta}{\partial z} \right] - \left(K_{33} - K_{11} \right) \sin\theta \cos\theta \left(\frac{\partial\theta}{\partial z} \right)^2 +$$
$$+ \left(\alpha_2 \sin^2\theta - \alpha_3 \cos^2\theta \right) \frac{\partial\upsilon}{\partial z} + \frac{\Delta\varepsilon\, E^2}{4\pi} \sin\theta \cos\theta = \gamma_1 \frac{\partial\theta}{\partial t} + I \frac{\partial^2\theta}{\partial t^2} ,$$ (2)

where θ is liquid crystal directors deformation angle, K_{11} and K_{33} represent the splay and bend Frank elastic constants,

$$\Delta\varepsilon = \varepsilon_\parallel - \varepsilon_\perp$$ (2a)

is the dielectric anisotropy,

$$E(z) = 4\pi \cdot D_z / \left(\varepsilon_\parallel \sin^2\theta + \varepsilon_\perp \cos^2\theta \right)$$ (2b)

is the electrical field in the LC layer, D_z is the z component of electrical displacement, υ is the flow velocity, α_i is the Leslie's viscosity coefficient [11], $\gamma_1 = \alpha_2 - \alpha_3$ is rotational viscosity, and I is the inertia moment. This equation is so complicated that no analytical solution has been obtained except for some computer simulation [12].

The problem simplifies greatly by neglecting the angular moment of inertia because γ_1 is so large that the change of orientation is strongly damped at all attainable electric field strengths. If inertial effects were appreciable, backflow would also mask a damped oscillatory motion of molecules.

In the small-angle orientation when the maximal angle of direction orientation $\theta_m < 50°$ [13] the backflow can be accounted for introducing effective viscosity for *"Splay"* (S-) and *"Bend"* (B-) deformations:

$$\gamma_S^{\,*} = \gamma_1 - 2\alpha_3^2 / \left(\alpha_3 + \alpha_4 + \alpha_6 \right),$$ (3a)
$$\gamma_B^{\,*} = \gamma_1 - 2\alpha_2^2 / \left(\alpha_4 + \alpha_5 - \alpha_2 \right);$$ (3b)

this is valid when $\partial\upsilon_x / \partial z \neq 0$.

Electric field is connected to applied voltage in thin layers by the relation

$$E \approx U / d .$$ (4)

In addition, let us assume the angular distribution in the cell is

$$\theta(z,t) = \theta_m(t) \cdot \cos(\pi z/d) ,$$ (5)

and $\theta(-d/2) = \theta(d/2) = 0$. If we substitute Eq. (4) into Eq. (2) and for approximation $\theta_m{}^4$ we can find (by analogue with [14] but for S-effect only)[1]

$$\theta_m^2 = \frac{\tau_2}{2\tau_1}\left(1 + \tanh\frac{t - \tau_0}{\tau_1}\right) ,$$ (6)

where

$$\tau_1 = \frac{\gamma_1{}^* d^2}{K_{11}\pi^2} \Big/ \left(\frac{U^2}{U_0{}^2} - 1\right) ,$$ (6a)

$$\tau_2 = \frac{\gamma_1{}^* d^2}{K_{11}\pi^2} \Big/ \left(\frac{2U^2}{3U_0{}^2} + K\right) ,$$ (6b)

$$K = (K_{33} - K_{11}) / K_{11} ,$$ (6c)

and

$$U_0 = \pi\sqrt{\frac{4\pi K_{11}}{\Delta\varepsilon}}$$ (7)

is the threshold voltage, and τ_0 is the integration constant. τ_0 is the necessary time for reorientation of liquid crystal molecules to exceed temperature fluctuation ones.

The modification of orientation under the influence of electrical field can happen in the "a" or "b" direction. It depends on the thermal fluctuation direction of domains. These fluctuations are much less than reorientation induced electrically, and they can be evaluated as the first order approximation in terms of θ. Here is the formula for thermal fluctuation:

$$\langle\Delta\Phi\rangle = \frac{\Delta\Phi_m}{2}\frac{d^2 R\rho T^o}{NM}\left(\frac{n_\parallel{}^2}{n_\perp{}^2} + \frac{n_\parallel}{n_\perp}\right)\left(\pi^2 K_{11} + \frac{\Delta\varepsilon U^2}{4\pi}\right)^{-1} ,$$ (8)

where R is the universal gas constant, ρ is density of the liquid crystal, T^o is thermodynamic temperature, N is the number of molecules in one domain, M is gram-equivalent of the liquid crystal. The detailed derivation can be found in [14]. When $U = 0V$, fluctuations are the largest. Monotone changing of $\Delta\Phi$ takes place non-immediately but after reorientation according to the voltage U_0, when

---

[1] We ignored another solution $\theta_m^2 = \frac{\tau_2}{2\tau_1}\left(1 + \coth\frac{t - \tau_0}{\tau_1}\right)$, because for $U > U_0$ and $t \to \infty$, the angle θ_m decreases, but as follows from experiments, the birefringence must be increasing.

the electric-induced turn became more than thermal fluctuations. Let us evaluate the thermal fluctuations value for the following parameters: $R = 8.31144j\cdot(mol\cdot K)^{-1}$, $\rho = 1g/cm^2$, $T^o = 293^oK$, $d = 5\mu$, $N = 10^6$, $M = 270g/mol$ and other parameters see Appendix A for LC999. When U is vanishing, $\langle\Delta\Phi\rangle = 1.68\cdot10^{-7}\pi$. With control voltage increase fluctuations' amplitude decreases and the parameter τ_0 becomes a negligibly small quantity. The more detailed research of fluctuations in nematic liquid crystal is given in [15].

The birefringence index of extraordinary light beam represents a projection of large axis of optical indicatrix on the initial orientation direction [16]

$$n(z) = \sqrt{\frac{n_\| n_\perp}{n_\perp^2 \cos^2\theta(z) + n_\|^2 \sin^2\theta(z)}} \, .$$

(9)

The integral value $n(z)$ can be represented as series

$$n(z) = n_\|\left[1 - \frac{a}{4}\theta_m^2 + \left(\frac{a}{16} + \frac{9a^2}{64}\right)\theta_m^4 - \dots\right] ,$$

(10)

$$a = (n_\|^2 - n_\perp^2) / n_\perp^2 .$$

Substituting Eq. (10) into Eq. (1) and taking into account Eq. (6) we obtain

$$\Delta\Phi = \Delta\Phi_m\left[1 - \frac{1}{8}\left(\frac{n_\|^2}{n_\perp^2} + \frac{n_\|}{n_\perp}\right)\frac{U^2 - U_0^2}{\frac{2}{3}U^2 + KU_0^2}\left(1 + \tanh\frac{t - \tau_0}{\tau_1}\right)\right],$$

(11)

here $\Delta\Phi_m$ is the largest value of phase delay when $n = n_\|$ in (1). For voltage $U > U_0$, phase retard $\Delta\Phi$ decreases with time constant τ_1 to the stationary state:

$$\Delta\Phi_0 = \Delta\Phi_m\left[1 - \frac{1}{4}\left(\frac{n_\|^2}{n_\perp^2} + \frac{n_\|}{n_\perp}\right)\frac{U^2 - U_0^2}{\frac{2}{3}U^2 + KU_0^2}\right].$$

(12)

The function $\Delta\Phi = \Delta\Phi_0(U)$ is represented in Fig. 2 by dotted line. Solid line shows the dependence from experiment. We used the parameters of liquid crystals from Appendix A. You can see the approximation by Eq. (5) is true for $(U - U_0)/U_0 < 1$. For higher voltage it is necessary to involve a collective contribution of many high-order modes in Eq. (5) [10].

For stationary case Eq. (2) has zero right part and the solution can be obtained in quadratures

$$(z')^2 \frac{U^2}{U_0^2} = \frac{d^2}{\pi^2}\int_{\theta_m}^{\theta'}\sqrt{\frac{1 + K\sin^2\theta}{\sin^2\theta_m - \sin^2\theta}}d\theta ,$$

(13)

where θ' is a director tilt angle at the distance z' from the layer center. The angle θ_m is fixed like a parameter. We can find the corresponding voltage U. Than we fixe this value U and calculate z' varying θ' from θ_m to θ_0 with a little constant step. The derived distribution $\theta = \theta(z)$ is substituted in Eq. (9) and the result in Eq. (1).

If now the voltage is switched off, the molecules come back to initial planar condition under the influence of elastic forces from the molecules attached to the cell walls. The relaxation time constant is

$$\tau_{off} = \tau_1 \big|^{U=0} = \frac{\gamma_1^* d^2}{K_{11}\pi^2} . \tag{12}$$

For the large signal approximation we can neglect the moments of elastic forces, which are much less than the rotating moment of electrical field, and Eq. (1) is reduced to the equation
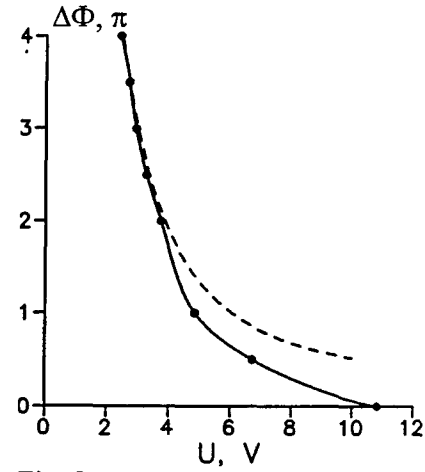

Fig. 2. Phase delay against rms voltage: solid line is the experimental dependence and dotted line is the dependence obtained from Eq. 12. The LC1001 layer has the thickness 5μ; λ=0.6328μ.

$$\frac{\Delta\varepsilon\, E^2}{4\pi}\sin(\theta)\cos(\theta) = \gamma_1^* \frac{\partial\theta}{\partial t} \tag{13}$$

with initial condition

$$\theta(z)\big|_{t=0} = \theta(z) . \tag{13a}$$

From Eq. (13) the required time for reorientation from $\theta > 0$ to θ_m. to is given by

$$t_r = \frac{\gamma_1^* d^2}{K_{11}\pi^2} \ln\frac{\tan\theta_m}{\tan\theta} \Big/ \left(\frac{U}{U_0}\right)^2 . \tag{14}$$

Although Eq. (6a) and Eq. (14) look alike, they are different. τ represents the rise time at $1/e$ of the directors' deformation angle which is different from t by definition.

The decay time can be obtained from reduced Eq. (2) using the approximation $K_{11} \approx K_{33}$

$$K_{11}\frac{\partial^2\theta}{\partial z^2} = \gamma_1^* \frac{\partial\theta}{\partial t} . \tag{15}$$

Taking into account Eq. (13a) we obtain [17]

$$\theta(z,t) = \frac{2}{d}\int_{-d/2}^{d/2}\left[\sum_{m=1}^{\infty}\theta(z')\sin\frac{\pi m z'}{d}\sin\frac{\pi m z}{d}\exp\left(-\frac{m^2 t}{\tau_{off}}\right)\right]dz' . \tag{16}$$

So, rapidity depends on

        a) viscosity and elastic constants,
        b) thickness of liquid crystal layer,
        c) control voltage.

7

We give a brief analysis of these factors.

2.1 Viscosity and elastic constants

Choosing a liquid crystal with low viscosity to increase the rate of cell response leads to the necessity of the control voltage increase. Since such crystals, as a rule, possess a small optical activity, a high degree of reorientation of the molecules is required for the same variation of the phase delay. This effect can be characterized approximately by the "reaction factor" $\gamma_1/\Delta n$ [18], where $\Delta n = n_\parallel - n_\perp$ is the optical anisotropy. However, viscosity γ_1 can be decreased by increasing temperature: $\gamma_1 \sim \exp(A/kT^\circ)$ where A is an activation energy [16], and k is the Boltzmann constant. But in this case elastic constant K_{11} is decreasing also: $K_{11} \sim S^2$ where S is the order parameter of the liquid crystal. The linear decrease of γ_1^*/K_{11} [see Eqs. (6a), (12) and (14)] is observed, when temperature is increased to some optimal temperature T_{opt}. Above T_{opt}, the elastic constant drops more significantly than the effective viscosity does, resulting in slower decay time [19].

Elastic constants' values depend on the method of orientation. In the case of planar orientation K_{ii} (i=1, 2, 3) are greater than in the tilted one, and the decay time is shorter [20].

2.2 Thickness of the liquid crystal layer

The liquid crystal layer thickness determines rapidity as $\sim 1/d^2$, therefore thin cells are preferable for fast phase modulation [21]. However, there are two problems. The first is a small depth of modulation which is more limited then given by Eq. (1). The second is high probability of breakdown or short circuit. In the real substrates the liquid crystal molecules surface alignment is seldom uniaxial due to the surface roughness, defects or irregular alignment treatments. The "virtually inactive" thickness is defined by the quality and preparation of the substrates. Under the conditions of strong anchoring and good surface quality, the thickness of the partially disordered surface layers is reduced. On the other hand, the large "virtually inactive" thickness is expected for weak anchoring and rough surface alignment. In [22] "virtually inactive" thickness is estimated as $\sim 0.3\mu$ for each surface, and in [21] an estimate of 0.5μ for the thickness of the inactive volume per cell is thus obtained.

We discuss the second problem in the next section.

2.3 Control voltage

Reorientation can be induced both by static and alternating electrical field. In the case of static fields the current must flow through the electrodes, so electrodes' processes become important. The electric field in the liquid crystal layer becomes inhomogeneous and is determined by anisotropy conditions. Double layers are formed at the electrodes, which decrease the field in the cell, so a higher applied voltage is needed to reorient the layer as in the case of alternating fields. In [23] it was found that the development of the double layers takes several seconds, so they can be completely neglected for alternating fields. In another paper [20] it was written that 10ms unipolar pulses cause polarization of liquid crystal and the increase of τ_{off} was connected with it.

Besides, low frequency control voltages can stimulate electro-hydrodynamical instability [24] when $\varpi < 1/\tau_e$ [16] where $\tau_e \approx \varepsilon_\parallel/4\pi\sigma_\parallel$ is the dielectric relaxation time, $\sigma_\parallel$ is specific conductivity. And conductive currents can simulate hysteresis [25].

In practice, in order to avoid ion displacements we shall use an alternating bipolar voltage of frequency greater then the carrier relaxation frequency. In the case of alternating field we assume the frequency to be high enough that the alignment of the molecules cannot follow the alternation of the field (typically>100Hz) but low enough, that the polarization can follow it (typically<10^6Hz).

One of the ways to increase rapidity is to use high control voltages. It was found that the rise time decreased on increase in the control voltage as U^{-2}.

There is a critical value 60V/μ [20] of the strong electrical field. To prevent probability of breakdown or short circuit the authors of [26] suggest placing all electrodes on the one substrate. The other substrate borders the homeotropic aligned liquid crystal layer with positive anisotropy. To avoid the critical value they increase a distance between electrodes and a liquid crystal layer had a very small thickness. This configuration allowed to use the control voltage 200V on the layer thickness 1.5μ and to obtain the rise time 0.4ms, and the decay time 5ms. The main imperfection of this configuration as a wavefront corrector is small spatial resolution because of a long distance between control electrodes.

3. LIQUID CRYSTAL MODULATORS' CONTROL METHODS

In this section we present the results of experimental studies of control methods using one-channel liquid crystal corrector. All measurements were performed in a laser interferometers with $\lambda=0.6328\mu$.

3.1 Amplitude control

The simplest method employs amplitude variation of rms (acting) voltage. Dependence $\Delta\Phi(U)$ is monotone, see Fig. 2. All evaluations of time parameters for this method have been performed in the previous chapter. In practice, for thin cells with typical values of $d \approx 5\mu$, $\gamma_1^* \approx 10...100$cP, $K_{11} \approx 10^{-6}$dyn, $U_0 \approx 1...5$V, $U \approx (1...100) \times U_0$, the range of "turn on" time is $25 \cdot 10^{-6}...0.8$s and "turn off" is $0.25...2.5$s. We used this method in our earlier works [27, 28].

3.2 Transient method

The idea of transient nematic liquid crystal effect [10] is to utilize the fast decay time due to the small relaxation angle because of highly deformed liquid crystal directors. The working principle of this fast modulation is illustrated in Fig. 3. For better understanding we used a liquid crystal modulator placed between two crossed polarizers and oriented at 45° to the polarization axes. A relatively high ac voltage is initially applied to the liquid crystal cell. As a result, almost all the molecules are aligned by the electric field almost orthogonal to the substrate surfaces except in the boundary layers. When these highly deformed directors start to relax, i.e., the voltage is removed completely, the directors undergo free relaxation. However, when the transmitted light intensity I reaches the first minimum, a voltage is applied to the cell to stop the directors' motion. Authors of [10] make difference between this mode of operation and bias voltage effect [29] (sometimes called surface mode), because bias voltage is constantly present during the relaxation process. The presence of this holding voltage provides an intermediate stopping force to the LC directors and, thus, decreases the relaxation time. In reality these effects have the same cause - bias voltage. Consider the control signal in the case of transient effect (Fig. 3c). The sequence of unipolar pulses has a "constant" component [30]

$$a_0 = \frac{2\tau}{T}V_0 \tag{17}$$

Variation of the pulse duration τ, period T or the voltage amplitude V_0 leads to the "bias" voltage change. When these parameters are constant, the "bias" voltage is constant too.
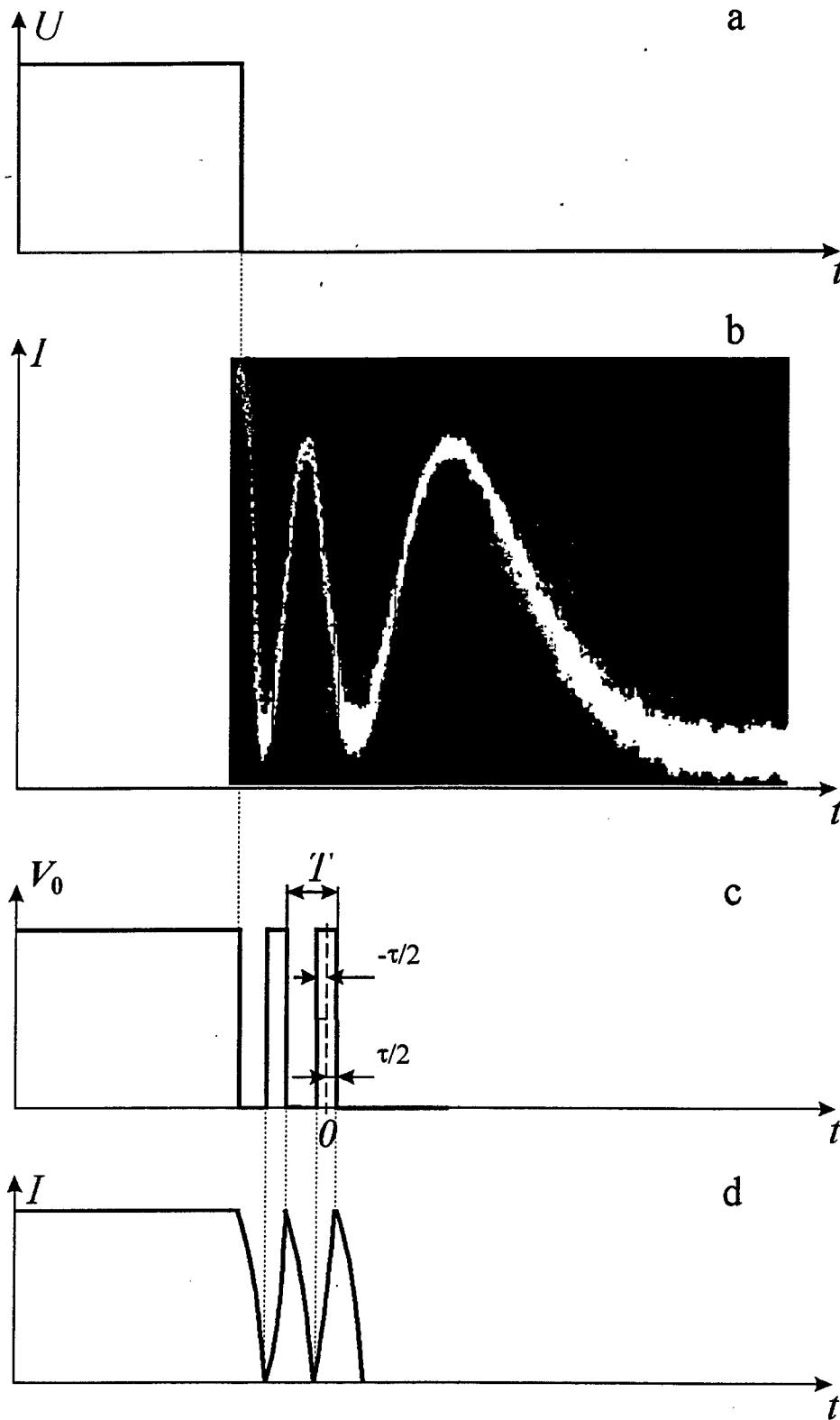
Fig. 3. Transient effect: (a) voltage pulse; (b) electrooptic response; (c) control voltage for periodical intensity modulation; (d) intensity modulation.

In [10] 1ms response time was mentioned. Authors of [29] obtained 0.16...0.2ms time for π modulation. They used bias voltage $U_b \approx 2U_0$ and dual-frequency control. We discuss the dual-frequency control method further in the special section.

10

3.3 Pulse method

We have named this method so because it can be implemented by means of pulse technique.

When we use bipolar rectangular control voltage we can drive a modulator by variation of pulse period-to-pulse duration ratio $q = T/\tau$. Amplitude of m harmonics is given by [30]

$$a_m = \frac{2V_0}{\pi m}\sin\left(m\pi\frac{\tau}{T}\right). \qquad (18)$$

When $T < 0.01$s birefringence depends on the acting voltage value and it does not depend on the voltage sign in this moment. The given voltage represents a number of harmonics and each harmonic makes its contribution in the birefringence magnitude. Variation of parameter q leads to harmonics' amplitude change and, consequently, to variation of phase modulation depth in liquid crystal layer. For example, the total effect from harmonics in cases "a" and "b" (Fig. 4) is different.
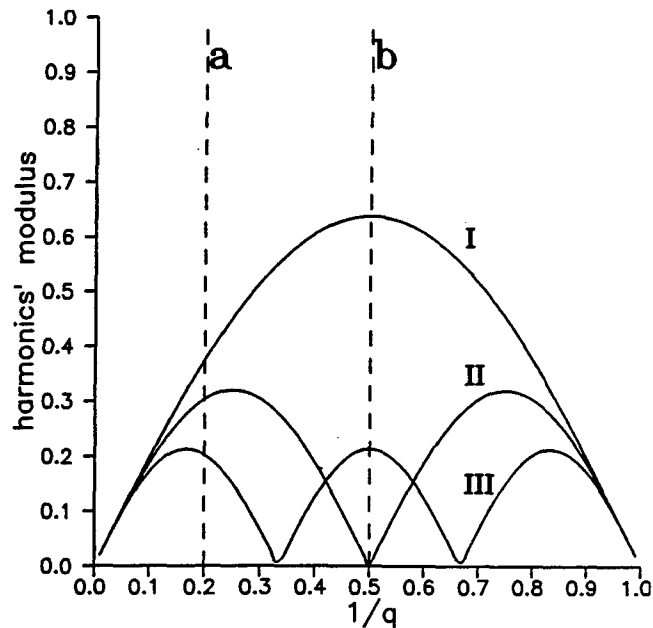
Fig. 4. Variation of harmonics' modulus as function of $1/q$; (I) first harmonic, (II) second harmonic, (III) third harmonic.

We first used this method for control of liquid crystals with a low-frequency sign inversion of the dielectric anisotropy [31]. A diagram of control voltage for that case is shown in Fig. 5, and experimental dependencies of phase delay versus $1/q$ are shown in Fig. 6. In our case variation of birefringence was connected also with ratio between switching on and switching off rates. However, the same control voltage can be used for birefringence control in usual liquid crystals. We have measured first and second harmonics of control voltage by the selective voltmeter to demonstrate that. Results are presented in Fig. 7. The control voltage generator circuit diagram is placed in Appendix B.
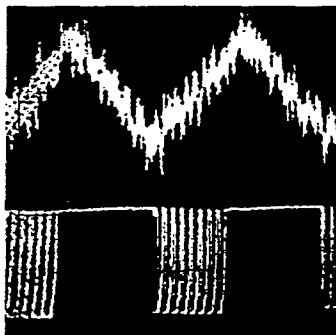
This method is of a great importance for the modal liquid crystal modulators control [32] because voltage form selection allows to decrease phase aberrations [33]. Modal liquid crystal wavefront correctors have distributed electrical parameters and high sensitivity to the control voltage spectrum. At present our team designs the aberration free adaptive lens, but this item exceeds the

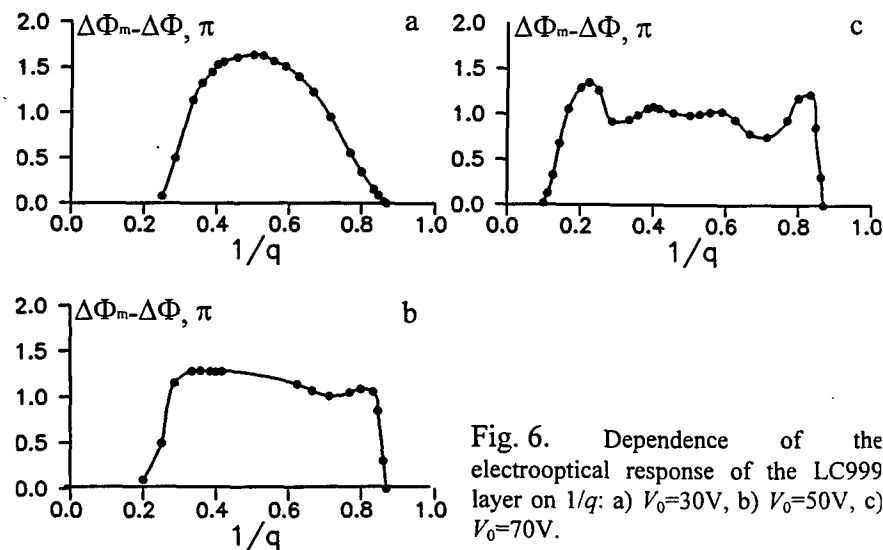Fig. 5. Liquid crystal electrooptic response to the dual frequency control voltage.

Fig. 6. Dependence of the electrooptical response of the LC999 layer on $1/q$: a) $V_0 = 30$V, b) $V_0 = 50$V, c) $V_0 = 70$V.
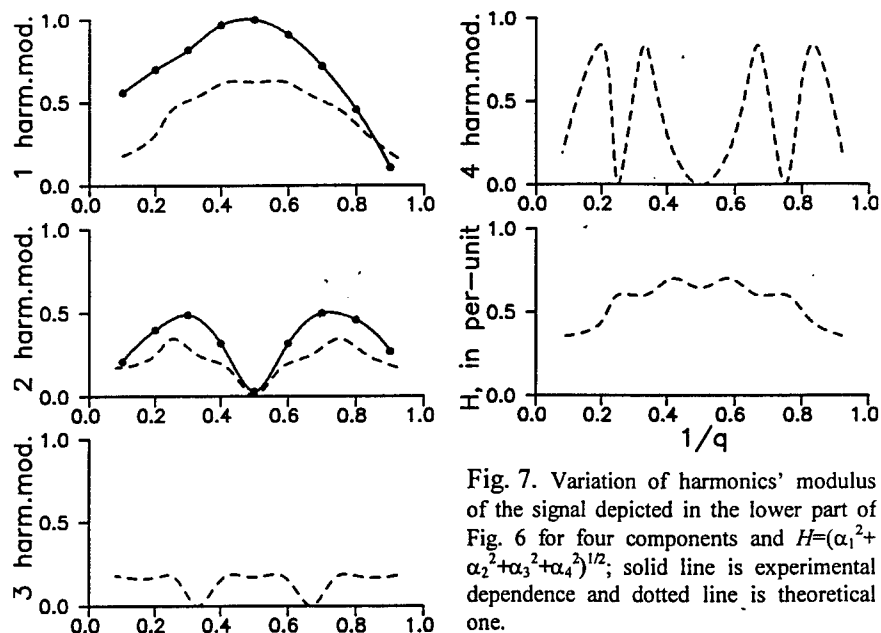
Fig. 7. Variation of harmonics' modulus of the signal depicted in the lower part of Fig. 6 for four components and $H=(\alpha_1^2+\alpha_2^2+\alpha_3^2+\alpha_4^2)^{1/2}$; solid line is experimental dependence and dotted line is theoretical one.

bounds of our contract.

3.4 Dual frequency control

The time t and the time constant τ_1 have minimal values for the large voltage amplitude and small thickness, whereas the decay time is independent of the voltage. It is possible to reduce τ_{off} if the anisotropy sign in the liquid crystals is inverted by forced relaxation in a high-frequency electric field when $\Delta\varepsilon < 0$.

The dielectric permittivities of all liquid crystals vary with the frequency of applied field when $f > 1/\tau_D \sim 10^8 Hz$ (τ_D is a relaxation time of isotropic liquid [16]). In the range of sound frequencies $\varepsilon_\parallel$ and $\varepsilon_\perp$ are usually constant (see, for example, characteristics of LC654 in Appendix A). However, for certain materials $\varepsilon_\parallel$ changes which leads to $\Delta\varepsilon$ sign change (see, for example, characteristics of LC999 and LC1001 in Appendix A). This is associated with relatively long molecules with molecular dipoles at an angle to long axis, notably the trinuclear diesters A_1-CO_2-A_2-CO_2-A_3 where A_1, A_2, A_3 represent substituted rings [18], e.g.

(19)
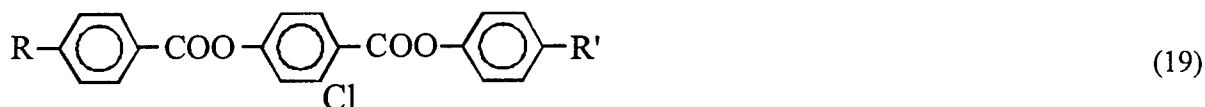
Dielectric permittivity $\varepsilon_\parallel$ is sensitive to reorientations of molecular dipole moments parallel to the major symmetry axis of the molecule. Such molecular reorientations are restricted by cooperative molecular interactions that are responsible for the stability of the liquid-crystalline state. Consequently, the value of $\varepsilon_\parallel$ varies with the frequency of the applied field.

For most liquid crystals $\Delta\varepsilon$ is positive at low frequencies of applied voltage and negative at high frequencies. The frequency at which $\Delta\varepsilon$ reverses sign is called the crossover frequency f_c. The sign reversal of $\Delta\varepsilon$ can be used to orient the liquid crystal either with the optic axis parallel ($\Delta\varepsilon > 0$) or normal ($\Delta\varepsilon < 0$) to the direction of electrical field by selecting the frequency of the applied voltage.

Two-frequency addressing first have been proposed for dynamic-scattering-type liquid crystal displays. The operation principle consisted in the transition from conductivity anisotropy regime to a dielectric anisotropy induced alignment regime at cut off frequency [34].

12

We regard here the usage of dual-frequency control to increase rapidity of liquid crystal wavefront correctors.

For the of the control voltage frequency below f_c and $U > U_0$ the electrooptical S-effect occurs. The S-orientation time τ_S is the same rise time as in the first chapter. For a voltage with frequency $f > f_c$, $\Delta\varepsilon < 0$ and molecules of liquid crystal orient perpendicular to the field. The B-effect occurs. The B-orientation time τ_B is determined in the same way as τ_S, but here instead K_{11} it is necessary to write K_{33}. The t_{off} value is comparable with the t_{on} and the first is determined by applied voltage as well. To decrease the phase delay by the quantity $\Delta\Phi$ it is necessary to apply a low-frequency voltage at the time $t_S=\Delta\Phi/\Phi_S'$ where $\Phi_S=\partial\Phi_S/\partial t$ is the S-effect rate. In order to increase the phase delay by the same quantity it is necessary to apply a high-frequency voltage at the time $t_B=\Delta\Phi/\Phi_B'$ where $\Phi_B=\partial\Phi_B/\partial t$ is the B-effect rate. The ratio between t_S and t_B determines the birefringent state of the liquid crystal layer in dynamics. The static value of $\Delta\Phi$ depends on harmonics of control voltage.

The dynamic electrooptic response to the dual frequency control voltage is represented in Fig[2]. 5. In our experiments we used liquid crystal cell with initial planar orientation. The layer thickness was 5μ, the active diameter of cell was 2cm, the low frequency was 1kHz and the high frequency was 18kHz.

The static dependence $\Delta\Phi(1/q)$ obtained by means of interferometer is shown in Fig. 6. The dependence $\Delta\Phi(1/q)$ is non-monotone, it repeats the sum of first harmonics' modulus. Higher harmonics are shunted by a modulator capacitance. By increasing voltage the curve $\Delta\Phi$ repeats the form of harmonics more precisely. Besides, there is nonlinear modulator capacitance dependence upon voltage and frequency (Fig.8). These circumstances complicate the feedback design. An adaptive system with a liquid crystal modulator belongs to nonlinear parametric tracking systems [35,36] and is
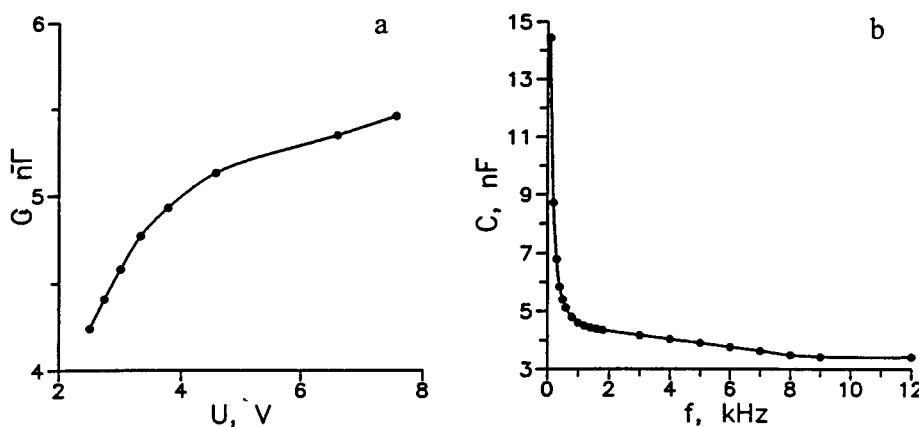

Fig. 8. Dependence of capacitance on applied voltage (a) and frequency (b).

too complex for full theoretical analysis. We are going to manufacture the special programmable high-voltage generator and to build the one-channel adaptive system. By control voltage form variation we shall try to maximize rapidity and steadiness. The description of electronic equipment is presented below.

Now we present two examples of analog control of the liquid crystal modulator in one-channel adaptive interferometer [37].

---

[2] Some time disparity between control voltage and electrooptic response connected with time delay $\sim 1/4f$ between electrooptic response and ac feeding voltage [20].

We have selected the modified Twyman-Green-Williams interferometer because it has convergent spherical beams and the influence of a beamsplitter cube quality on interferogram quality is negligible. The interferometer setup including the liquid crystal cell is shown in Fig. 9. The liquid crystal cell had been manufactured on the beamsplitter cube [38] *3*. The reference mirror *4* mounted on the piezoelectric actuator introduces the model alteration of optical path length difference (interferometer working point displacement). An error signal in the feedback circuit is determined as a result of comparison between the photoelectric voltage from the photoelectric cell (PEC) *8* onto which interference fringes are projected and the reference steady voltage by the comparator *C* (Fig. 10). The reference voltage is equal to the PEC signal amplitude when the mirror actuator voltage is zero. The interference fringes move along the PEC window. If the PEC signal amplitude is greater than the reference voltage, the logical unit appears at the comparator output and the high-frequency impulses from the generator *G* pass through the 2AND-NO element. If the PEC signal is less or equal to the reference voltage, the logical unit voltage appears at the 2AND-NO through the transistor gate *K* and differential *RC* chain (in order to prevent the liquid crystal molecular dissociation by the dc influence) across the liquid crystal cell. The values of *R* and *C* are chosen so as to avoid by-pass of the liquid crystal cell at the frequency $f \gg 1/RC_{LC}$ and to obtain maximum bandwidth of error signal $C \gg C_{LC}$. In the experiment the capacitance C_{LC} range was from 3.7 to 6.7nF, *R* was equal to 10kOhm and *C* to 1µF.
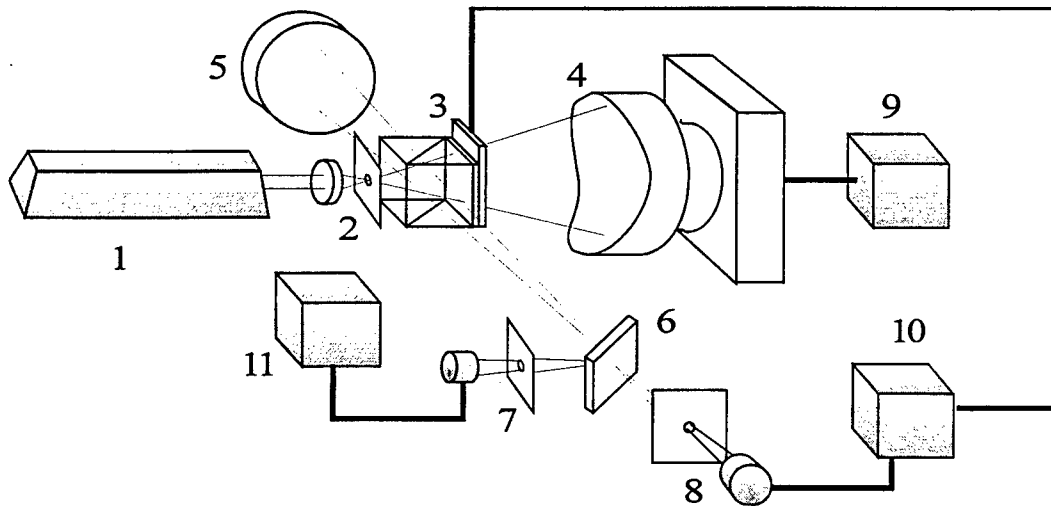

Fig. 9. Stabilized interferometer including LC cell: (1) He-Ne laser; (2) microobjective and pinhole; (3) beamsplitter cube with LC cell; (4) subject spherical mirror mounted on piezoelectric actuator; (5) reference spherical mirror; (6) semitransparent mirror; (7, 8) photoelectric cells with diaphragms; (9) special signal form generator; (10) servoelectrononics; (11) spectrum analyzer.

In the approximation $\Phi'_S \approx \Phi'_B = \Phi'$ and without allowance for the region of insensitivity of the system, the phase difference of the light beam $\Phi(z,t)$ is found from the equation
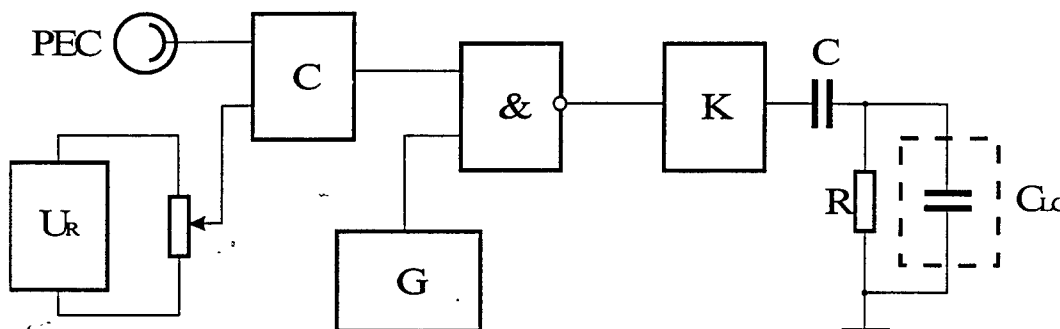

Fig. 10. Feedback loop for phase conjugation system. PEC - photoelectric cell, C - comparator, G - generator, & - 2AND-NO, K - transistor gate, U_R - source of reference voltage.

14

$$\Phi + [\text{sgn}(u) - 1(u)]\, t_0 \Phi' = \Phi_0 \ , \tag{20}$$

where

$$\text{sgn}(u) = \begin{cases} 1, & u>0 \\ 0, & u=0 \ , \\ -1, & u<0 \end{cases} \tag{20a}$$

$$1(u) = \begin{cases} 1, & u = 0 \\ 0, & u \neq 0 \end{cases} , \tag{20b}$$

$\Phi_0 = 2\pi z_0 / \lambda$ is the phase difference corresponding to the reference voltage, z_0 is the desired path difference, $u = \cos(\Phi) - \cos(\Phi_0)$, and $t_0\Phi'$ is the system sensitivity. Solving this equation for any phase difference deviation δ from the desired one we obtain

$$\Phi = \Phi_0 - \delta \exp\{[\text{sgn}(u) - 1(u)]\, t / t_0\} . \tag{21}$$

Since phase is 2π degenerated the Φ_0 value is obtained regardless the direction of the interference pattern movement across the PEC aperture. The phase difference $\Phi(z,t)$ oscillates with the period $2t_0$ and the amplitude $t_0\Phi'$. In the experiment the period of oscillations was 0.52ms and the amplitude was 0.09rad (λ=0.633µ). This is the property of relay tracking systems [36], and this way of feedback organization is well known as the phase conjugation method [39].

The degree of external influence suppression on the path length difference characterizes the efficiency of stabilization in the interferometer, and the suppression coefficient is a quantitative value of the efficiency

$$Q = 20 \log(U_+ / U_-). \tag{22}$$

Here U_- and U_+ are the signals' amplitude from the additional PEC 7 when the feedback is opened and closed, respectively. The measurement is performed by a spectrum analyzer 11 at the oscillator frequency of the constant amplitude 0,62π (Fig. 11). This value of oscillations was selected to provide the constant amplitude of mirror displacement by frequency variation. Fig. 12 demonstrates the process of suppression of 1kHz vibrations in the stabilized interferometer.
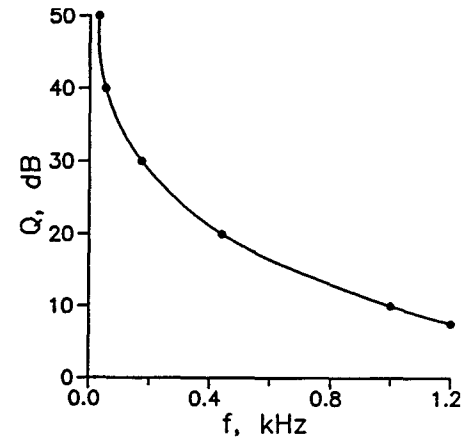

Fig. 11. External perturbations suppression coefficient in phase conjugation system.

We noted the non-monotonicity of $\Delta\Phi(1/q)$. This circumstance affects the steadiness of the system. The feeding voltage was selected carefully to prevent bistable or stochastic regimes. Most of the voltage variation range corresponds to unstable conditions.

Another scheme was more steady but more slow. Its block diagram is shown in Fig. 13. The presence of small high-frequency probe perturbations of wavefront and a significant range of light beam phase control in the frequency region of the external phase fluctuations are typical for adaptive optical systems operating on the basis of the aperture probing principle. The high frequency modulation was produced by the feeding voltage shown in Fig. 5 but had small amplitude. This voltage was formed by

15

the control block CB and the sine-wave generator G tuned to the frequency ω. The circuit diagram of the control block is represented in Appendix C. Thus the liquid crystal cell introduced the oscillations with the depth $a \ll \pi$ and with the frequency ω. The amplitude of the first harmonic after the filter F, which is tuned to ω, is equal to

$$U_F = -2\chi I_0 \sin(\delta) J_1(a) \sin(\omega t),$$

(23)

where χ is the PEC conversion efficiency, I_0 is the largest intensity in interference pattern and $J_1(a)$ is the first order Bessel function. The voltage U_F is multiplied by the reference voltage from generator G with the help of phase detector PD and the result is filtered at low frequency

$$U_{FD} = -\chi I_0 J_1(a) \sin(\delta).$$

(24)

From this equation it follows that the voltage U_{FD} can serve as the mismatch phase difference signal $\delta = \Phi - \Phi_0$. The increase of the system's astatism is achieved by introducing integrator I into the feedback loop. After integrator the error signal

$$U_1 = -\frac{h}{T_I} \chi I_0 J_1(a) \int \sin(\delta) dt$$

(25)

is fed to control block CB; T_1 is the integrator time constant and h is its gain coefficient.

Fig. 12. Suppression of 1kHz sine external perturbations : a) feedback off, b) feedback on.

For example, for the change in the phase difference $\delta = \Psi \sin(\Omega t)$ introduced by the reference mirror, where $\Psi < \pi$ and Ω is the oscillation frequency of the mirror, the first order approximation gives

$$U_I = \frac{U(\Psi)}{T_I \Omega} \cos(\Omega t),$$

(26)

where $U(\Psi) = 2\chi h I_0 J_1(\Psi)$.

Control block modulates the amplitude of the periodic sequence of high and low frequency pulses

$$U_{CB} = (U_{max} - \beta U_I) s(t),$$

(27)

where U_{max} is the largest pulse amplitude in the liquid crystal modulator, β is the control block gain coefficient, and $s(t)$ is the signal which produces the high-frequency modulation of the phase delay (Fig. 5).

For low frequency oscillations of the reference mirror $\Omega \ll \nu$ the voltage after differentiating circuit varies in phase opposite to δ

$$U_{LC} = \left[U_{max} \exp(-\nu t) - \beta \frac{U(\Psi)}{T_I \sqrt{\Omega^2 + \nu^2}} \sin(\Omega t - \Theta) \right] \cdot s(t),$$
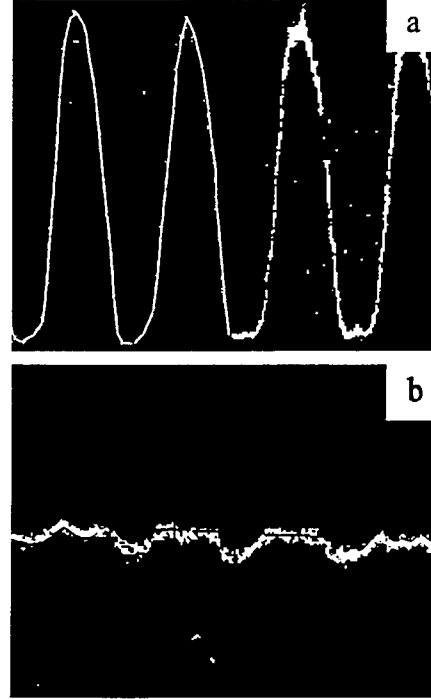
(28)

16

where $v = [R(C_{LC} + C)]^{-1}$, $\Theta = \arctan(\Omega/v)$.

Phase advance of the error signal is manifested only at high frequencies. This leads to an increase of the stability of the system but to a decrease of the depression coefficient [40].
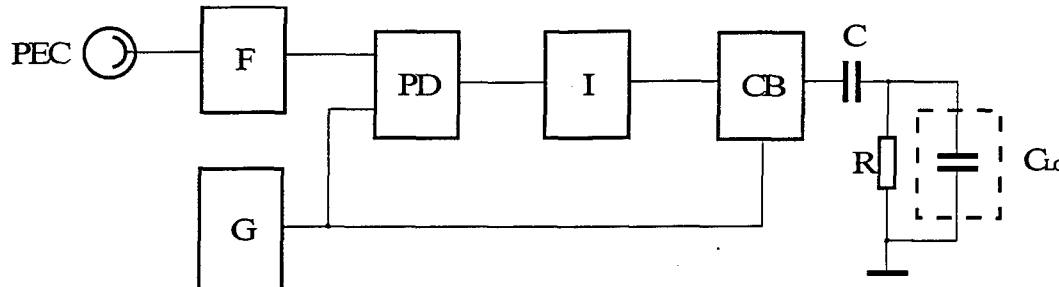

Fig. 13. Feedback loop for the aperture probing system. PEC - photoelectric cell, F - filter, G - generator, PD - phase detector, I - integrator, CB - control block.

In the experimental setup ω was equal to 1kHz. The filter F was tuned to the frequency 1kHz and had a transmission bandwidth of the ±100Hz. The time constant of integrator was chosen to be 0.56ms for the feedback loop sensitivity of 2V/π (not taking into account the gain of the control block). The depression coefficient dependence on the sinusoidal oscillations frequency of the reference mirror at the oscillations amplitude Ψ=2.5π is shown in Fig. 14.

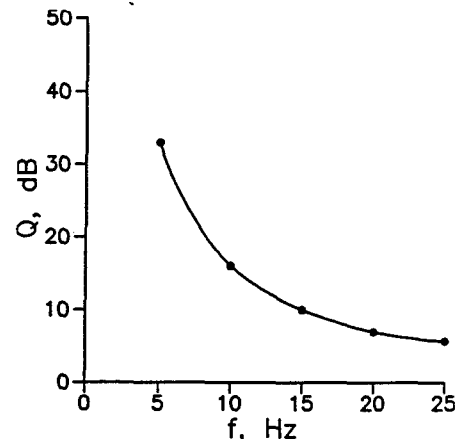In experiment we also observed the light scattering at the instant of control voltage frequencies switching. However, the false error signal was not registered because it had the frequency beyond the transmission bandwidth of the feedback loop. The scattering can limit the rapidity of adaptive systems. Authors of [41] in case of twist electrooptic effect observed the similar scattering. We are going to study the dynamic scattering influence.

Fig. 14. External perturbations suppression coefficient in system with aperture probing.

Theoretical limit of rapidity for liquid crystal modulators is the value $1/f_c$. Heating can shift this value. For example, in the [29] was obtained the rapidity 15...18μ for $T°$=42C, U_b=2U_0, U=220V. The cross frequency was shifted to 100kHz. One of the more obvious problems is that of the low capacitative reactance of the cell at high frequencies. It had been overcame by incorporation of the modulator into a parallel turned circuit, resonant at the high frequency used, so that the driving electronics sees the dynamic resistance of the circuit. To prevent the inductor shunting the cell at the low frequency, a blocking capacitor, whose reactance is negligible at the high frequency, was connected in series with the inductor.

In fast adaptive systems the control is much complicate because of it is necessary to vary the relation t_S/ t_B in according to the error signal. It leads to harmonics' variation of feeding voltage and to non-control birefringence variation. We hope to solve this problem by controlling the voltage time history and we design the special programmable generator for this purpose. In addition to we are going to linearize liquid crystal modulator response by harmonics' control and to increase stableness and rapidity of liquid crystal adaptive systems.

4. CONFIGURATION OF ELECTRONIC EQUIPMENT

Configuration of electronic equipment is represented in Fig. 15. This equipment consists of signals' generator adapter *GAD*, a photoreceiver adapter *RAD*, a digital-to-analog converter block *BDAC*. The generator adapter and the photoreceiver one are manufactured in IBM PC standard. They are placed in the computer inside and are connected with a system bus immediately. These elements have exterior plugs *X1* and *X2*. The digital-to-analog converter block is manufactured as a separate device. It is connected to appropriate adapters by cables for transmission of digital signals through plugs *X3* and *X4*. The liquid crystal modulator and the measuring photo-diode *PR* are connected to plugs *X5* and *X6* by coaxial cables.
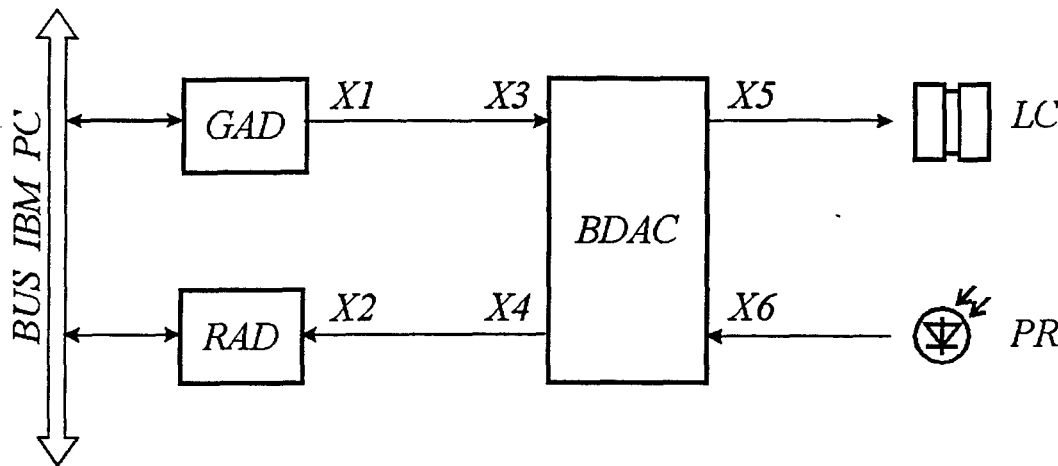

Fig 15.

4.1 The signals' generator adapter

This device is intended for generating of control voltage as digital codes and synchronization signals. Control voltage function shape is set by array, which contains 1024 references of 8-digit codes. Time slice between references is equal 4µs. It allows to set controlling function in 4ms time slice about. Block diagram of the generator adapter of signals is represented in Fig. 16. It contains a pilot signals' decoder of the system bus *DC*, an entering data register *IN-RG*, an output data buffer register *OUT-RG*, a memory addresses' counter *AC*, a buffer memory *RAM* by 1kb capacity, a control circuit *CS*. Output signals of the buffer register *OUT-RG DATA* and the signals of synchronization *KDR* and *STB* are removed in the exterior plug *X1*. The synchronization signal of frame *KDR* synchronizes beginning and extremity of generated data array. Indexing array cells of generated data corresponds to addressing meshes of the buffer *RAM*. Synchronization signals *STB* correspond to separate array cells of data. The control circuit *CS* allows to organize adapter use in the following conditions:

- move of file from the computer to the buffer adapter *RAM*;
- multiple cyclical reading of file from the buffer *RAM* in a *DATA* turnpike;
- test of the adapter *RAM*.

Schematic diagram of the adapter is represented in Fig. 1 of Appendix D. The adapter control is carried out through input-output ports by programming:

- OUTPUTPORT (310H) - reception of data in the register *IN-RG*;
- OUTPUTPORT (311H) - reset of the address counter;
- OUTPUTPORT (312H) - entry of data byte in the *RAM*;
- OUTPUTPORT (313H) - connection of the buffer *RAM* to the computer;

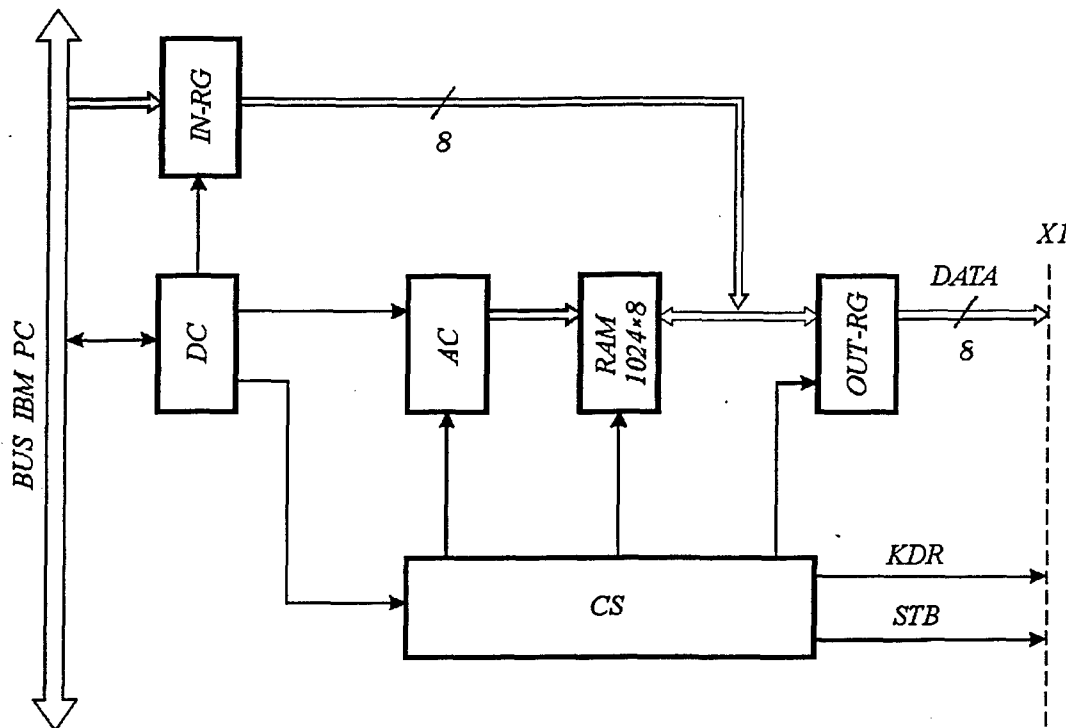- OUTPUTPORT (314H) - condition of cyclical reading of data in the plug *X1*.

Fig. 16. Block diagram of generator adapter of signals *GAD*.

In the adapter there is a possibility to change temporal parameters of control signals for the liquid crystal modulator by means of switches.

4.2 The photoreceiver adapter

This device is intended for registration of dynamic digital signals from the photoreceiver in the buffer *RAM* and input of its in the computer under control of exterior synchronization signals. Block diagram is represented in Fig. 17. The adapter contains a pilot signals' decoder of system bus *DC*, an entering register *RG-IN* and an output register *RG-OUT*, a addresses' counter *RAM AC*, a buffer *RAM* by 1kb capacity, a control circuit. Information register inputs *IN-RG*, synchronization signals' ones *KDR1* and *STB1* are connected to the exterior entering plug *X2*. The adapter is synchronized by frame impulse *KDR1* and reference clock pulse *STB1*. The control circuit *CS* allows to organize the adapter operation in the following conditions:

- move of data from the entering plug in the buffer *RAM*;
- reading of data from the buffer *RAM* in the computer;
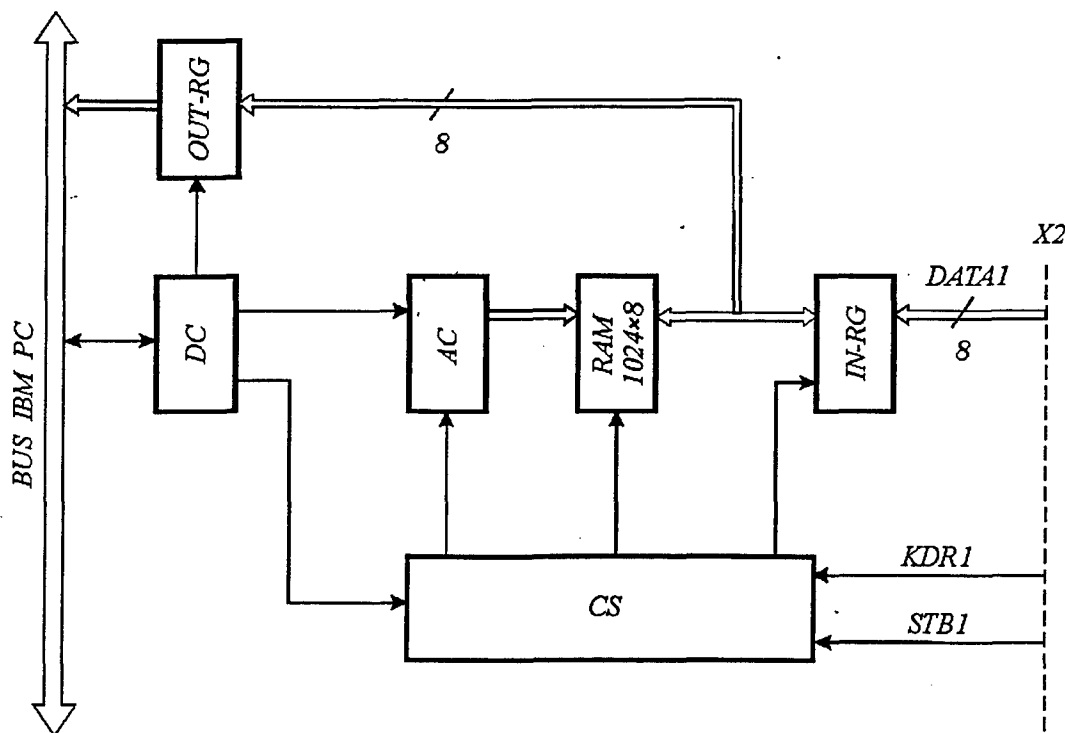- test of the adapter *RAM*.

Fig. 17. Block diagram of photoreceiver adapter *RAD*.

Schematic diagram of the adapter is represented in Fig. 2 of Appendix D. The adapter control is carried out through ports of input-output by programming:

- INPUTPORT (120H) - start of the adapter to data entry;
- INPUTPORT (121H) - reset of the address counter;
- INPUTPORT (122H) - reading of byte of data from *RAM* in the buffer register RG-OUT;
- INPUTPORT (123H) - input of status word of the adapter in the computer;
- INPUTPORT (124H) - input of byte of data in the computer.

The temporal performances of signals *KDR1* and *STB1* correspond to generator adapter signals *KDR* and *STB*.

4.3 Block of digital-to-analog converters

This device is intended for transformation of digital signals from the generator adapter into analog form and amplification its, and also digitization of signals from the photo diode. Block diagram is represented in Fig. 18 and schematic diagram is shown in Fig. 3 of Appendix D. The block contains a digital-to-analog converter *DAC*, a high-voltage amplifier *HVA*, an analog-to-digital converter *ADC*, an photo diode signals' amplifier *A* and a control circuit *CS*. The signal from an exit of the generator adapter through the plug *X3* acts to an input of the digital-to-analog converter *DAC*. Voltage is transformed to a range from -10V up to +10V in the exit *DAC*. The high-voltage amplifier increases this signal to a range from -125V up to +125V. The given analog signal is passed through the plug *X5* to the liquid crystal modulator. The control circuit *CS* synchronizes the analog-to-digital converter and the photo diode voltage amplifier by means of signals *KDR* and *STB*. Output code from the analog-to-digital converter is passed in the plug *X4*.
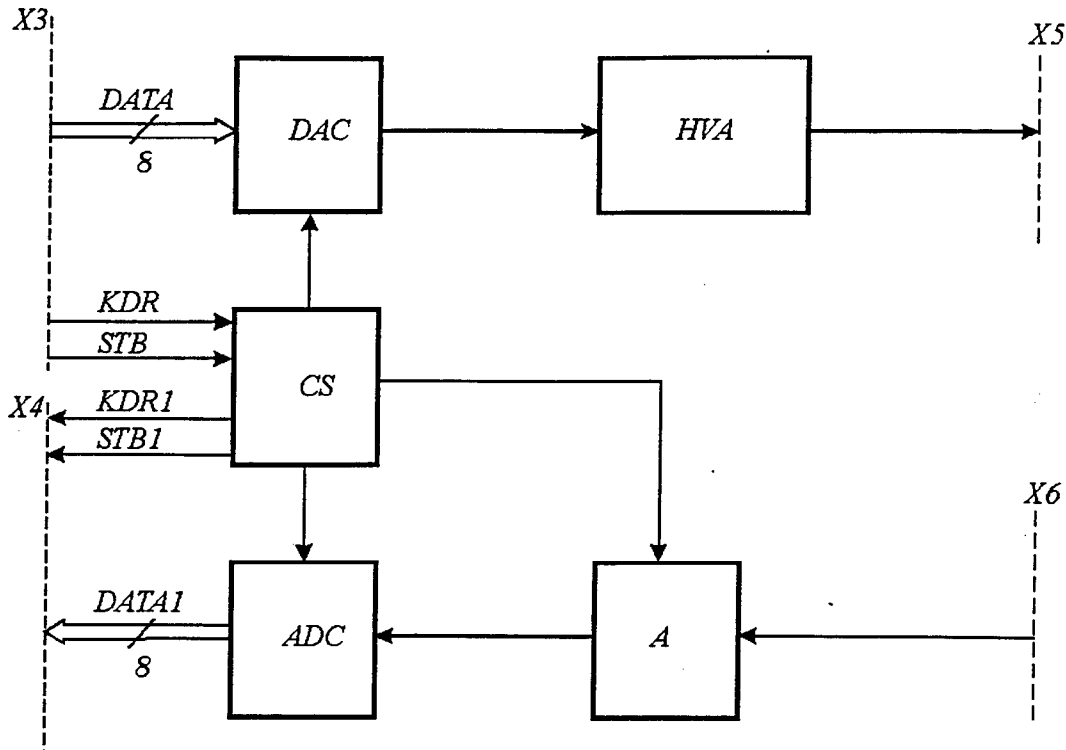
Fig. 18. Block diagram of digital-to-analog converter block *BDAC*.

4.4 The high-voltage amplifier

The most complicated element of the electronic equipment is the high-voltage amplifier *HVA*. Its parameters should correspond the following values:

- voltage amplitude $|U| \geq 125V$;
- maximal frequency $f \geq 150$ kHz.

In order to obtain these signal parameters the amplifier should have the slew rate of output voltage $S = 2\pi Uf \geq 115V/\mu s$. The high-voltage amplifier that matches these parameters is the operational amplifier of model 3584 by "BURR BROWN" firm . It has the following parameters for resistive impedance:

- output voltage range from -140V up to +140V;
- slew rate - 150 V/μs;
- maximal output current $I_m = 15mA$.

Liquid crystal modulator impedance is capacitance $C \sim 4nF$ for 1kHz frequency and it is changed by frequency and voltage (Fig. 8). If the liquid crystal modulator is connected with amplifier output directly, the slew rate is $dU/dt = I_m /C = 3.75V/\mu s$ and the buffer current amplifier is necessary. Its gain coefficient is given by $K = (115V/\mu s)/(3.75V/\mu s) \approx 30.7$

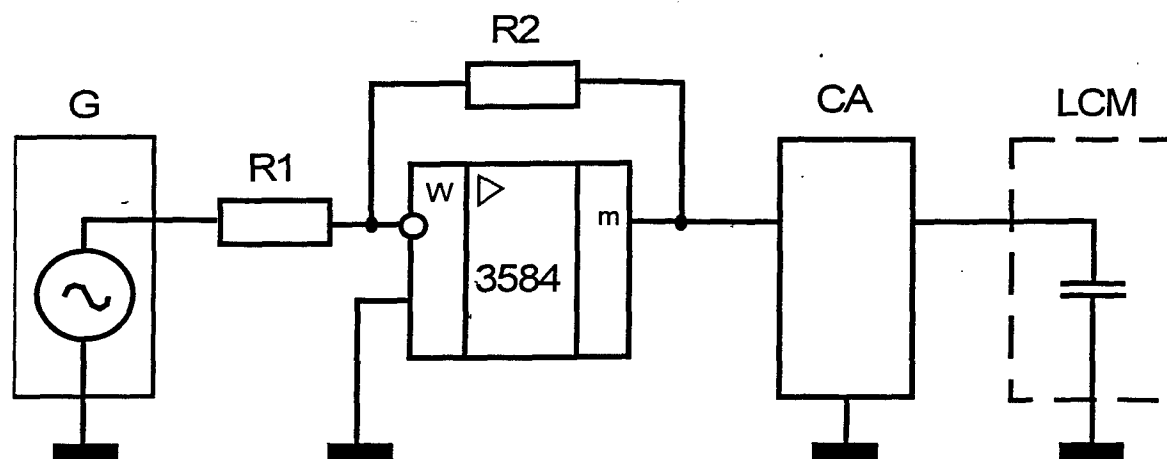Thus, block diagram shown in Fig. 19 have been chosen as the high-voltage amplifier *HVA*.

Fig. 19. Block diagram of high-voltage amplifier H*VA*.

REFERENCES

1. Z..U.Gotra, L.K.Vistin', V.V.Parhomenko, L.M.Smerklo, E.P.Dzisjak, V.T.Fechan, "Indicator devices on liquid crystals", Moscow, "Soviet radio", 240 p. (1980), rus.
2. W.P.Bleha, "Progress in liquid crystal light valves", Laser Focus/Electro-Optics, October, pp.111-120 (1983).
3. S.D.Jacobs, K.A.Cerqua, K.I.Marshall, A.Schmid, M.J.Guardalben, K.J.Skerrett, "Liquid-crystal laser optics: design, fabrication, and performance", Jornal of the Optical Society of America B, Vol.5, No.9, pp.1962-1979 (1988).
4. N.A.Riza, "Liquid crystal-based optical control of phased array antennas", Journal of Lightwave Technology, Vol.10, No.12, pp.1974-1984 (1992).
5. I.Kompanets, A.Andreev, E.Pozhidaev, "Properties of new FLC and prospects of their application in fast optical valves, SLM and displays", Proceeding of SPIE, Vol.2754, (1996).
6. I..Abdulhalim, "Continuous phase-only or amplitude light modulation using ferroelectric liquid crystals with fixed boundary orientations", Optics Communications, Vol.108, No.1, pp.219-224, (1994).
7. S.E.Broomfield, M.A.A.Neill, E.G.S.Paige, "Programmable multiple-level phase modulation that uses ferroelectric liquid-crystal spatial light modulators", Applied Optics, Vol.34, No.29, pp.6652-6665 (1995).
8. G.D.Love, "Liquid crystal phase modulator for unpolarized light", Applied Optics, Vol.32, No.13, pp.2222-2223 (1993).
9. D.W.Berreman, "Dynamics of liquid-crystal twist cells", Applied Physics Letters, Vol.25, No.1, pp.12-15 (1974). "Erratum: Dynamics of liquid crystal twist cells [Appl.Phys.Lett.25, 12 (1974)]", Applied Physics Letters, Vol.25, No.5, p.321 (1974).
10. S.T. Wu, Chiung-Sheng Wu, "Small angle relaxation of highly deformed nematic liquid crystals", Applied Physics Letters, Vol.53, No.19, pp.1794-1796 (1988).
11. W.H. de Jeu, "Physical prperties of liquid crystalline materials" , Moscow, "World" publ., 152p. (1982), rus. *or Gordon and breach science publishers, 1980.*
12. V.G.Chigrinov, "Software package for simulation of electrooptical & optical characteristics of LC-displays", Version 12.1N (1994).
13. V.G.Chigrinov, V.V.Belyaev, "Temporal characteristics of oriented electrooptic effects in nematic liquid crystals", Crystallography, Vol.22, No.2, pp.603-607 (1977), rus.
14. G.Labrunie, J.Robert, "Transient behavior of the electrically controlled birefringence in a nematic liquid crystal", Journal of Applied Physics, Vol.44, No.11, pp.4869-4874 (1973).
15. A.Yu.Valkov, V.P.Romanov, "Fluctuation and scattering of light in nematic liquid crystals", Journal of Experimental and Theoretical Physics, Vol.83, No.5, pp.1777-1787 (1982), rus.

16. L.M.Blinov, "Electro- and magneto-optics of liquid crystals", Moscow, "Science" publ., 384p. (1978), rus or "Electro-Optical and Magneto-Optical Properties of Liquid Crystals", Wiley, New York (1983).

17. P.D.Berezin, I.N.Kompanets, V.V.Nikitin, S.A.Pickin, "The orienting effect of an electric field on nematic liquid crystals", Journal of Experimental and Theoretical Physics, Vol.64, No.2, pp.599-607 (1973), rus.

18. M.G.Clark "Dual-frequency addressing of liquid crystal devices", Microelectron Reliability, Vol.21, No.6, pp.887-900 (1981).

19. S.T. Wu, "Phase retardation dependent optical response time of parallel-aligned liquid crystals", Journal of Applied Physics, Vol.60, No.5, pp.1836-1838 (1986).

20. F.L.Vladimirov, I.E.Morichev, L.I.Petrova, N.I.Pletneva, "Light modulators based on fields effects in nematic liquid crystals", Optical-mechanical industry, No.5, pp.11-13 (1987), rus.

21. U.Efron, S.T.Wu, T.D.Bates,"Nematic liquid crystals for spatial light modulator: recen studies", Journal of the Optical Society of America B, Vol.3, No.2, pp.247-252 (1986).

22. S.T. Wu, U.Efron, "Optical properties of thin nematic liquid crystal cells", Applied Physics Letters, Vol.48, No.10, pp. 624-626 (1986).

23. L.Bata, A.Buka, J.Janossy, "Reorientation of nematic liquid crystal films by alternating and static fields", Solid State Communications, Vol.15, No.3, pp.647-649 (1974).

24. W.S.Quon, E.Wiener-Avnear, "Transient laser phenomena in nematic liquid crystals subject to ac electric fields", Applied Physics Letters, Vol.24, No.11, pp.529-531 (1974).

25. H.J.Deuling, W.Helfrich, "Hysteresis in the deformation of nematic liquid crystal layers with homeotropic orientation", Applied Physics Letters, Vol.25. No.3, pp.129-130 (1974).

26. F.L.Vladimirov, E.A.Morozova, "Features of electro-optical replay of nematic liquid crystal with positive dielectric permittivity in transverse electrical field", Optical-mechanical industry, No.10, pp.61-62 (1989), rus.

27. A.F.Naumov, "Wavefront correctors based on liquid crystal transparencies", in the collection "Holography methods in science and technique", Leningrad, "Academy Science of USSR, A.F.Ioffe's Physical-Technical Institute" publ., pp.216-221 (1985).

28. A.A.Vasil'ev, A.F.Naumov, V.I.Shmal'gausen, "Wavefront correction by liquid-crystal devices", Soviet Journal of Quantum Electronics, Vol.16, No.4, pp.471-474.

29. V.V.Belyaev, A.A.Vasil'ev, I.N.Kompanets, A.A.Matsvejko, A.V.Parfenov, Yu.M.Popov, "Increasing of rapidity of liquid crystal light modulators", Letters to Journal of Technical Physics, Vol.6, No.14, pp.845-847 (1980), rus.

30. I.S.Gonorovsky, "Radio-technical circuits and signals", Moscow, "Soviet Radio" publ., 671p. (1971), rus.

31. A.A.Vasil'ev, A.F.Naumov, S.A.Svistun, V.G.Chigrinov "Pulse control of a phase corrector liquid crystal cell", Letters to Journal of Technical Physics, Vol.14, No.5, pp.397-400 (1988), rus.

32. A.F.Naumov "Modal Wavefront Correctors", Proceeding of P.N.Lebedev Physical Institute, Vol.217, pp.177-182 (1993), rus.

33. S.P.Kotova, M.J.Loktev, A.F.Naumov, A.V.Parfenov, T.N.Sapsina, "The control of liquid crystal phase transmission", Bulletin of Samara University, Vol.4, N2, pp.167-173 (1996), rus.

34. T.S.Chang, E.E.Loebner, "Crossover frequencies and turn-off time reduction scheme for twisted nematic liquid crystal displays", Applied Physics Letters, Vol.25, No.1, pp.1-2 (1974).

35. F.P.Jarkov, V.A.Sokolov, "Circuits with variable parameters", Moscow, "Energy" publ., 223p. (1976), rus.

36. V.A.Dorezyuk, A.F.Naumov, V.I.Shmal'gauzen "Control of liquid-crystal correctors in adaptive optical systems", Journal of Technical Physics, Vol.59, No.12, pp.35-41 (1989); rus.

37. E.P.Popov, "Non-linear systems theory of automatic regulation and control", Moscow, "Science" publ., 255 p. (1988), rus.

38. M.A.Vorontsov, J.D.Dumarevskij, S.V.Kolobkov, A.N.Malov, A.F.Naumov, V.I.Shmal'gauzen "Stabilizated interferometer", patent 1404811 A1, 04/14/1986.

39. M.A.Vorontsov, V.I.Shmal'gauzen, "Principles of adaptive optics", Moscow, "Science" publ., 335p. (1985), rus.

40. P.H.Hammond, "Feedback theory and its applications", Moscow, "GIPML", 423p. (1961), rus. *or London, English Universities Press, (1958).*

41. V.V.Tsvetkov, V.B.Fyodorov, V.A.Tsvetkov, M.N.Fyodorova, "A study of licuid crystal light polarization plane switches on basis of the twist effect with two-frequency control", Quantum electronics, Vol.7, No.11, pp.2306-2312 (1980), rus.

42. L.A.Sena, "Units of physical values and its dimensions", Moscow, "Science" pudl., 336p. (1977), rus.

APPENDIX A

Liquid crystal materials reference data produced by Liquid Crystal Materials and Technologies of Organic Intermediates & Dyes Institute

LC materials	LC654	LC999	[3]LC1000	LC1001
$T_{smelting}$, °C	0	-3		-14
$T_{enlightenment}$, C (the phase transition tem.)	+66	+79		+85.4...+86.8
[4] Specific electric conductivity $\sigma_{\parallel}$, $Ohm^{-1}cm^{-1}$	$<10^{-10}$	$<6 \cdot 10^{-10}$ for T°=20°C, f=200Hz		
Dielectric parameters for T°=20°C (for LC1001, T°=25°C)	$\varepsilon_{\perp}$=+6.5 $\Delta\varepsilon$=+10.7	$\varepsilon_{\perp}$=+7.4, $\Delta\varepsilon$=+2.1 , f=200Hz $\Delta\varepsilon$=-2.2 , f=40kHz		$\varepsilon_{\perp}$=+7.1, $\Delta\varepsilon$=+2.5 , f=500Hz $\Delta\varepsilon$=-2.2 , f=40kHz
Crossover frequency f_c , kHz for T°=20°C	no	8.5		7.0
Refraction coefficients for λ=589nm, T°=20°C	$n_{\perp}$=1.536, Δn=0.2	$n_{\perp}$=1.537, Δn=0.24		$n_{\perp}$=1.5335, Δn=0.25
Viscosity η_2, cP for T°=25°C	27	36.4		
Threshold voltage U_{90},V	1.6 for T°=25°C, thickness 10μ	3.3 for T°=22°C, thickness 12μ		3.7 for T°=22°C, thick.10μ, f=1kHz
Satiation voltage U_{10},V	2.2 for T°=25°C, thickness 10μ	4.8, for T°=22°C thickness 12μ		5.5, for T°=22°C thickness 10μ, f=1kHz
Switching times, mc	$\tau_{growing}$=180 τ_{fall}=90 for T°=25°C, $\tau_{growing}$=1200 τ_{fall}=600	$\tau_{growing}$=0.15 τ_{fall}=0.25 for T°=22°C, U_l=U_h=80V[*)],		

---

[3] At this moment we have no data about this material.

[4] The record of dimension $Ohm^{-1} \cdot cm^{-1}$ is not correct although often met. In calculations it is necessary to convert it to sgs $^{-1}cm^{-1}$ or $Ohm^{-1}m^{-1}$, where 1Ohm = $9 \cdot 10^{11}$sgs [42].

	for T°=0°C, U=3V, thickness 10μ	thickness 12μ		
Modulus K_{33}/K_{11}				1.185

The switching times measurements were performed in periodic regime with 50Hz frequency modulation (Fig. 1). Pulse duration of low and high frequencies were 7.5mc and 0.7mc for LC999.
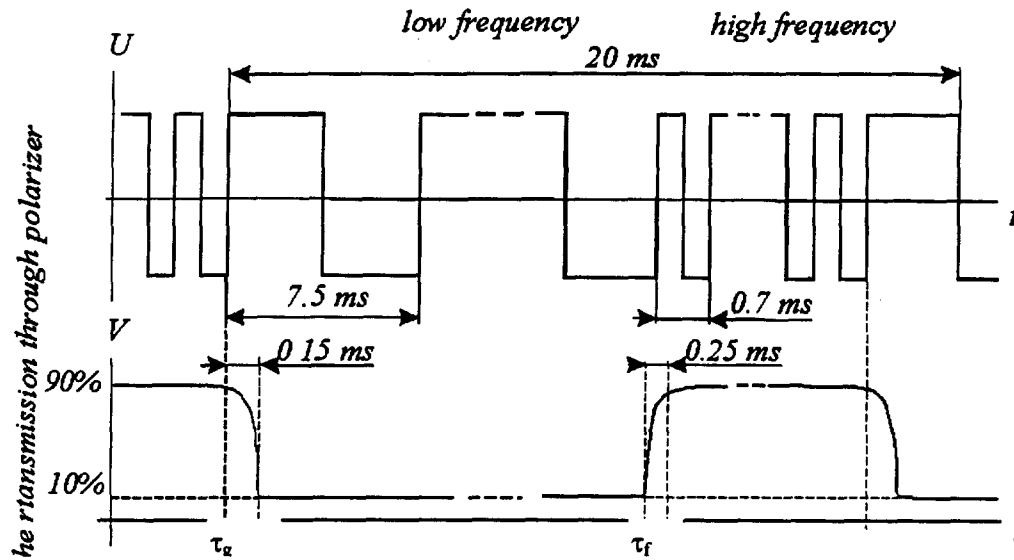

Fig. 15

APPENDIX B

Parametric stabilizer (*VT1, VD3, R8*) feeds low-voltage circuit elements. The assigning low-frequency generator with regulation of q is designed in terms of the integrated timer *NE555* (chip *DA1*). A q regulation range is from 5 % up to 95 %. Output signal of master clock is a modulation signal for operation of a more high-frequency generator, which have been manufactured in terms of DA2 multivibrator standard circuit. Resulting opposite phase signals from exits of DD1 chip operate optronic pairs DA3, DA4, which form a required two-polar signal to control of the light liquid crystal modulator.
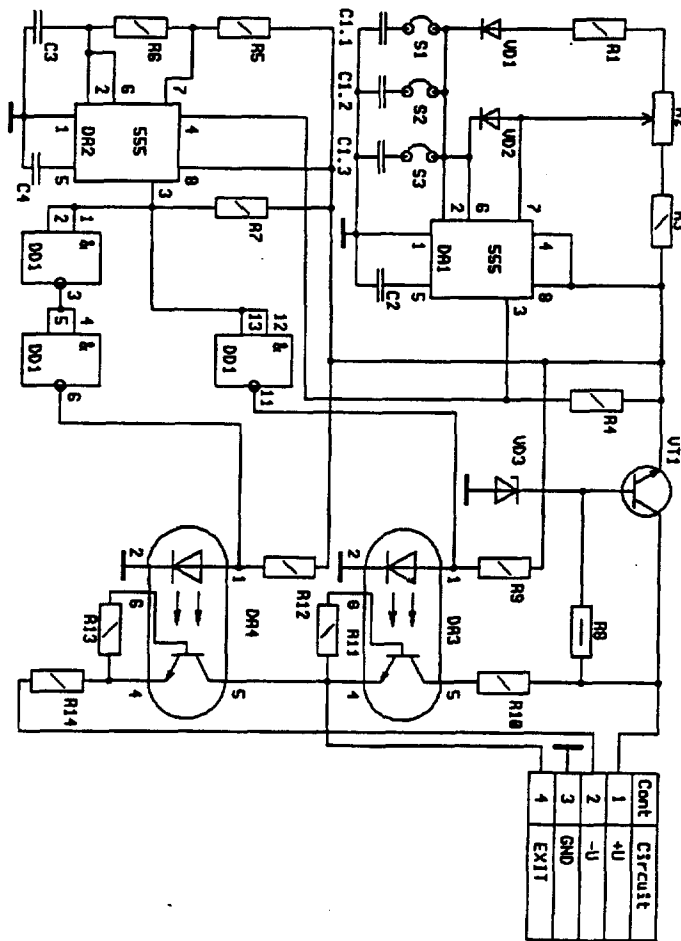
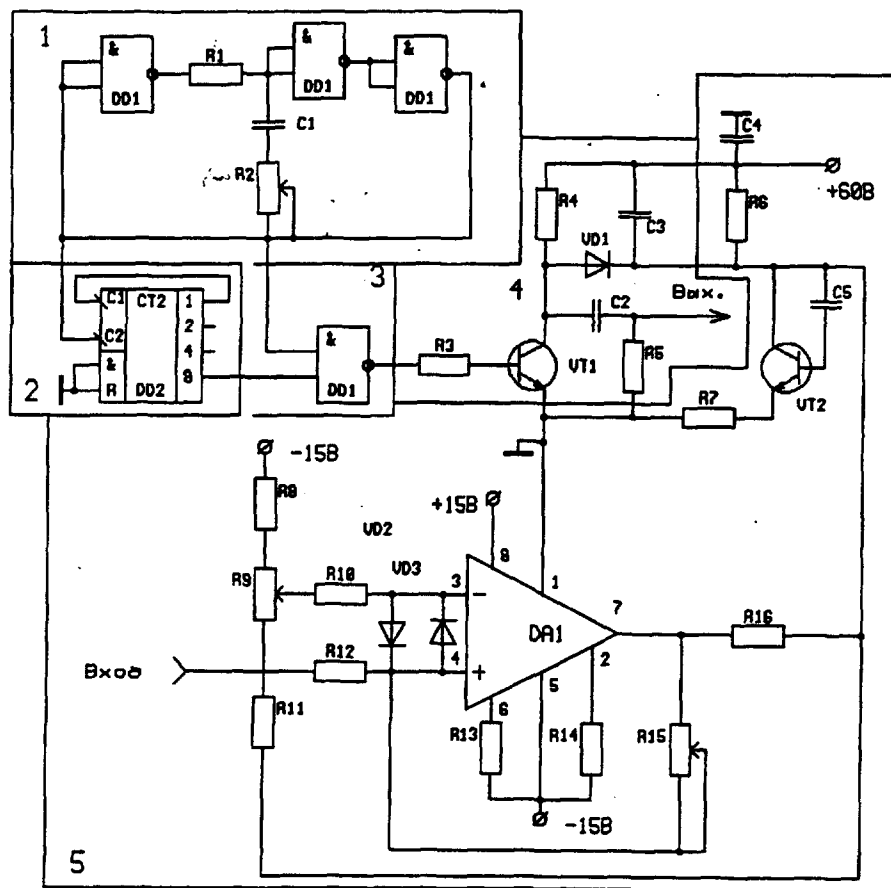Fig. 1. Controlled generator of two-polar rectangular pulses

APPENDIX C

Fig 1. Schematic diagram of control block: (1) rectangular pulse generator, (2) devisor frequency, (3) commutator, (4) gate, (5) limiter.
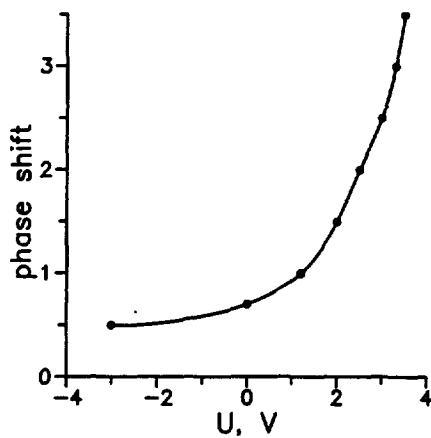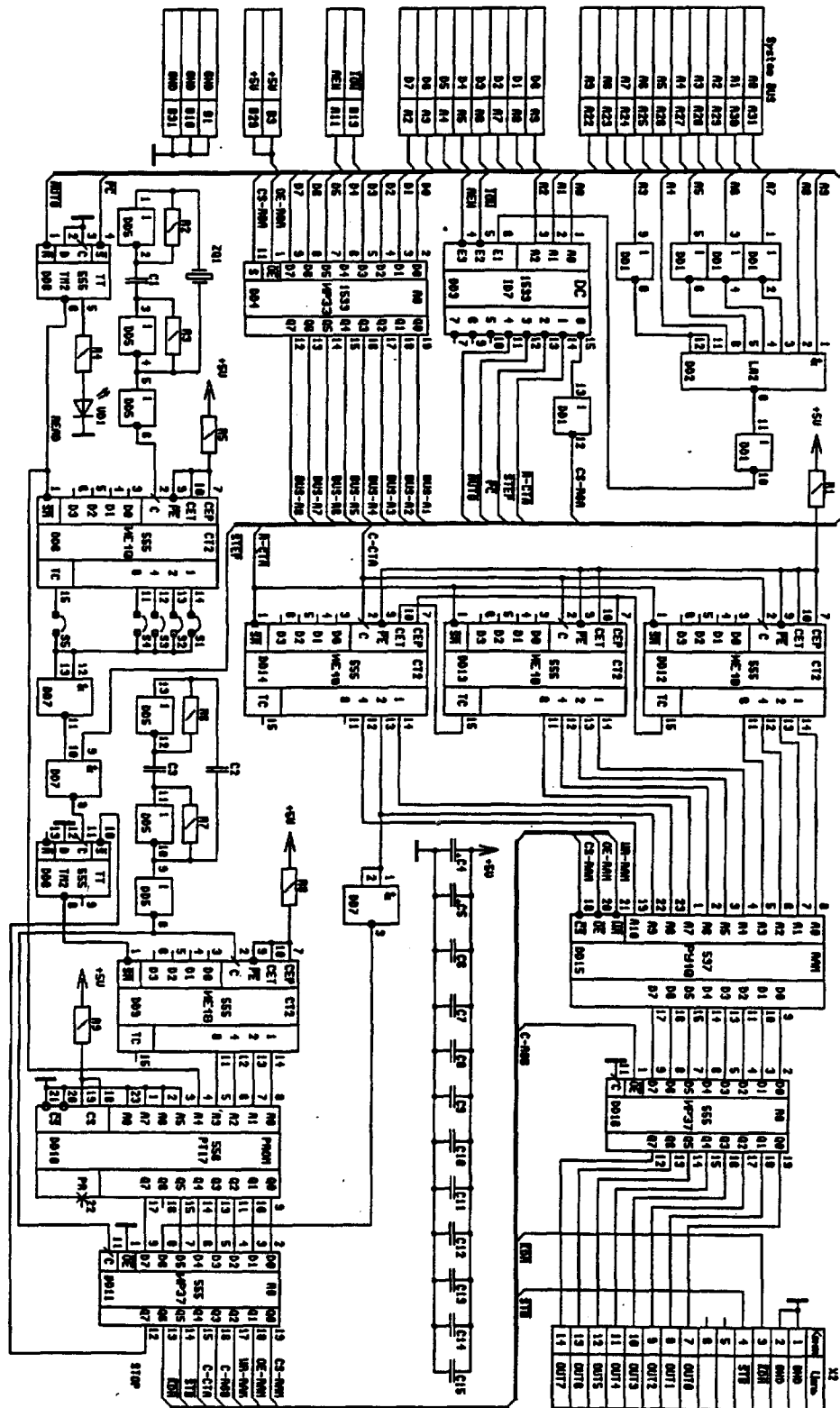

Fig. 2. Phase-voltage characteristics of control block; phase shift is $(\Delta\Phi_m - \Delta\Phi/\pi)$.

APPENDIX D

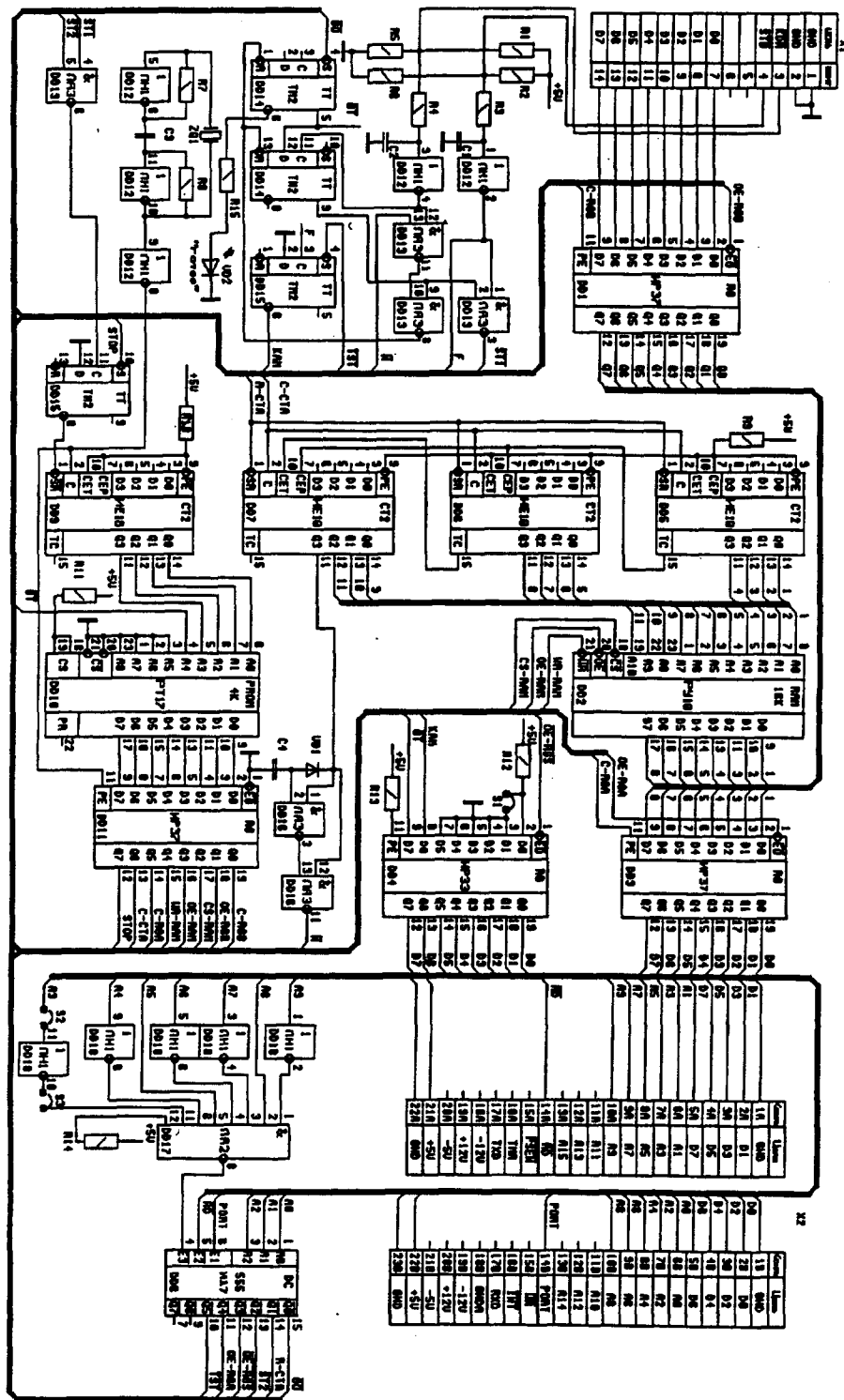Fig. 1. Schematic diagram of signals' generator adapter *GAD*.

Fig. 2. Schematic diagram of photoreceiver adapter *RAD*.

Fig. 3.Schematic diagram of digital-to-analog converter block
BDAC.